Eur. Phys. J. C (2023) 83:727
https://doi.org/10.1140/epjc/s10052-023-11845-9

THE EUROPEAN PHYSICAL JOURNAL C

Regular Article - Theoretical Physics

Masses and magnetic moments of exotic fully heavy pentaquarks

Wen-Xuan Zhang[1,a], **Hong-Tao An**[2,b], **Duojie Jia**[1,3,c]

[1] Institute of Theoretical Physics, College of Physics and Electronic Engineering, Northwest Normal University, Lanzhou 730070, China
[2] School of Physical Science and Technology, Lanzhou University, Lanzhou 730000, China
[3] Lanzhou Center for Theoretical Physics, Lanzhou University, Lanzhou 730000, China

Received: 23 June 2023 / Accepted: 14 July 2023 / Published online: 14 August 2023

Abstract Inspired by the observation of a resonant state $X(6600)$ of fully charm tetraquark by the CMS experiment of LHCb Collaboration in double J/ψ decay channel, we perform a systematical study of all configurations of fully heavy pentaquarks $P_{Q_1Q_2Q_3Q_4\bar{Q}_5}$ $(Q_i = c, b, i = 1, 2, 3, 4, 5)$ in their ground states in unified framework of MIT bag model. The color-spin wavefunctions of pentaquarks, classified via Young tableau and presented in terms of the Young–Yamanouchi bases, are used to compute masses and magnetic moments of fully heavy pentaquarks via numerical variational method, predicting a set of masses ranging from 8.229 GeV for the $P_{ccccc\bar{c}}$ to 24.770 GeV for the $P_{bbbbb\bar{b}}$. Combining with computed masses of fully heavy mesons and baryons, we find that masses of fully heavy hadrons(mesons, baryons, tetraquarks and pentaquarks) with identical flavor rise almost linearly with the number of valence quarks in hadrons, being consistent with the heavy quark symmetry in the heavy-quark limit.

1 Introduction

Possible existence of multiquark hadrons like tetraquarks $(q^2\bar{q}^2)$ and pentaquarks $(q^4\bar{q})$ was suggested earlier at the birth of quark model [1,2]. Later in the 1970s, multiquark states are studied by Jaffe via the MIT bag model [3,4]. Since observation of the $X(3872)$ [5] in 2003 by the Belle, many candidates of tetraquarks have been observed, some of which, such as the $Z_c(3900)$ [6] and the $T_{cc}(3875)$, are undoubtedly exotic. In 2020, a first candidate of fully charm tetraquark, the $X(6900)$/the $X(6600)$, has been observed by LHCb in the di-J/ψ invariant mass spectrum and later confirmed by CMS and ATLAS of the LHC at CERN [7–9]. For experimental searches of light-flavor pentaquark hadrons, it has been a long and nontrivial history, with no undisputed candidates found in over 50 years. Convincing evidence for pentaquark-like structures $P_c(4450)^+$ and $P_c(4380)^+$ with a minimal quark content of $uudc\bar{c}$ was reported by LHCb in a study of $\Lambda_b^0 \to J/\psi p K^-(J/\psi \to \mu^+\mu^-)$ decays [10] in 2015, for which the former peak(state) $P_c(4450)^+$ was resolved further into two states $P_c(4440)^+$ and $P_c(4457)^+$ (over 5.4σ) in 2019. More recently, LHCb collaboration reported evidences of two new charmonium pentaquarks with strangeness, $P_{cs}(4459)$ [11], in the $J/\psi\Lambda$ distribution(in $\Xi_b^- \to J/\psi\Lambda K^-$ decays) in 2021 and $P_{\psi s}^{\Lambda}(4338)$ [12], in flavour-untagged $B^- \to J/\psi\Lambda\bar{p}$ decays in 2022. After observation and measurement of two P_c states, many theoretical groups explained the $P_c(4450)^+$ and $P_c(4380)^+$ states as compact pentaquarks with diquarks and triquarks as building blocks [13–19], except for some few attempts via full five-body dynamics [20] which lead to states below the lowest threshold for spontaneous dissociation. On the other hand, there are molecular picture, proposed [21–24] before the first LHCb results [10], which interprets these narrow P_c states in terms of deuteron-like loosely bound states of the baryon and meson, such as the $\Sigma_c\bar{D}^{(*)}$ states. This picture favors the narrow P_c states, which have measured widths about 6–10 MeV for $P_c(4457)^+$ as well as $P_c(4312)^+$ and about 21 MeV for $P_c(4440)^+$, while the compact picture attributes narrow width to spin-orbit interaction (via spatial separation of c and $\bar{c}$ quarks). As the observed state $P_c(4380)^+$ is wider (with width about 205 MeV), the issue of width suppression remains to be explored. Till now, there are different pictures and approaches employed to analyze the hidden-charm pentaquarks (P_c and P_{cs}) [25–42], the hidden-strange and hidden-bottom pentaquarks [43–46]. One can infer Refs. [47,48] for the pre-2019 reviews and Refs. [49,50] for recent reviews. The purpose of this work is to systematically

[a] e-mail: zhangwx89@outlook.com
[b] e-mail: anht20@lzu.edu.cn
[c] e-mail: jiadj@nwnu.edu.cn (corresponding author)

study all possible ground-states of fully heavy pentaquarks, $P_{Q_1Q_2Q_3Q_4\bar{Q}_5}$ ($Q_i = c, b, i = 1, 2, 3, 4, 5$) in unified framework of MIT bag model. For this, we construct all color-spin wavefunctions of pentaquarks based on $SU(2)_s \times SU(3)_c$ group, classified via Young tableau and expressed in terms of the Young–Yamanouchi bases, to compute masses and magnetic moments of fully heavy pentaquarks in ground states and thereby predict their masses. With the help of numerical variation upon the bag radius, the chromomagnetic mixing among the color-spin configurations are explored in details. Computing further spin-independent masses of the mesons, baryons and tetraquarks all made of identical heavy flavors, we find a linear dependence of the hadron mass upon the heavy quark number N in hadrons. This linear rise of hadron masses is notable for the bottom sector and is demonstrated analytically via a variational method of bag model, being consistent with heavy quark effective theory (HQET) in heavy quark limit. After introduction, the wavefunctions of the fully heavy pentaquarks with various configurations are classified in Sect. 2 by the Young tableau and expressed in terms of the Young–Yamanouchi bases. In Sect. 3, we briefly review basic relations of MIT bag model including magnetic moments for each spin state, and describe how to apply the variational method to solve the bag model for the heavy hadrons. In Sect. 4, we perform numerical analysis of mass and magnetic moment for fully heavy pentaquarks. Similar computation are given to fully heavy mesons and baryons to show a linear relation for these fully heavy hadrons in Sect. 5. The paper ends with summary and conclusions in Sect. 6.

2 Wavefunctions of fully heavy pentaquarks

Fully heavy pentaquarks $P_{Q_1Q_2Q_3Q_4\bar{Q}_5}$ may contain two or more identical particles in the component $Q_1Q_2Q_3Q_4$, for which the corresponding parts of the wavefunctions have to be antisymmetric due to Pauli principle and colorlessness of $P_{Q_1Q_2Q_3Q_4\bar{Q}_5}$. Consider the pentaquark $P_{cccb\bar{b}}$, for instance. Since the component ccc in $P_{cccb\bar{b}}$ are identical in flavor, the antisymmetry requirement for a fermionic hadron (color singlet) implies that the wavefunction of $P_{cccb\bar{b}}$ has to be antisymmetric in orbital, color and spin under exchange of each cc pair among the component ccc. To respect the overall symmetry of the hadronic wavefunctions mentioned above, we utilize the Young tableau to represent the irreducible representations (bases) of the permutation group and thereby classify the pentaquark configurations with certain symmetry. For a given classification, we use the Young–Yamanouchi basis, which corresponds to the Young tableau, to construct explicitly the configuration describing the pentaquark we consider.

First of all, we consider color wavefunctions of the pentaquark $P_{Q_1Q_2Q_3Q_4\bar{Q}_5}$, which are singlets in color space. Utilizing direct product of the fundamental (color) representations $[3]_c$ and $[\bar{3}]_c$, one can classify, in the language of group theory, the color wavefunctions of a pentaquark as below:

$$\begin{aligned}
&[[3]_c \otimes [3]_c \otimes [3]_c \otimes [3]_c] \otimes [\bar{3}]_c \\
&= [(1_c \oplus 8_c \oplus 8_c \oplus 10_c) \otimes 3_c] \otimes \bar{3}_c \\
&\to (1_c \otimes 3_c \otimes \bar{3}_c) \oplus (8_c \otimes 3_c \otimes \bar{3}_c) \oplus (8_c \otimes 3_c \otimes \bar{3}_c) \\
&\to (3_c \otimes \bar{3}_c) \oplus (3_c \otimes \bar{3}_c) \oplus (3_c \otimes \bar{3}_c),
\end{aligned} \tag{1}$$

in which the allowed color singlet is $\{3_c \otimes \bar{3}_c\}$ only.

One is then forced to consider the color triplet in the direct product, $[[3]_c \otimes [3]_c \otimes [3]_c \otimes [3]_c]$, of the component $Q_1Q_2Q_3Q_4$, which corresponds to Young tableau [2,1,1] expressed by

$$\big[(12)_6\, 34\big]_3 = \begin{array}{|c|c|}\hline 1 & 2 \\ \hline 3 \\ \cline{1-1} 4 \\ \cline{1-1}\end{array}\,, \quad \big[(12)_{\bar{3}}\, 34\big]_3 = \begin{array}{|c|c|}\hline 1 & 3 \\ \hline 2 \\ \cline{1-1} 4 \\ \cline{1-1}\end{array}\,,$$
$$\big[(123)_1\, 4\big]_3 = \begin{array}{|c|c|}\hline 1 & 4 \\ \hline 2 \\ \cline{1-1} 3 \\ \cline{1-1}\end{array}\,. \tag{2}$$

Here, the subscript labels the irreducible representation of the color group $SU(3)_c$. This yields three color-singlet configurations of $P_{Q_1Q_2Q_3Q_4\bar{Q}_5}$ if one combines each of color-triplets (3_c) listed in Eq. (2) with the antitriplet ($\bar{3}_c$) of the remaining antiquark $\bar{Q}_5$. We express the Young tableau representing the obtained colorless configurations as

$$\begin{array}{|c|c|}\hline 1 & 2 \\ \hline 3 \\ \cline{1-1} 4 \\ \cline{1-1}\end{array} \otimes \bar{5} \quad \phi_1^P\,, \quad \begin{array}{|c|c|}\hline 1 & 3 \\ \hline 2 \\ \cline{1-1} 4 \\ \cline{1-1}\end{array} \otimes \bar{5} \quad \phi_2^P\,, \quad \begin{array}{|c|c|}\hline 1 & 4 \\ \hline 2 \\ \cline{1-1} 3 \\ \cline{1-1}\end{array} \otimes \bar{5} \quad \phi_3^P\,, \tag{3}$$

and correspond them to the following color wavefunctions explicitly:

$$\begin{aligned}
\phi_1^P = \frac{1}{4\sqrt{3}}\Big[&(2bbgr - 2bbrg + gbrb - gbbr + bgrb - bgbr \\
&- rbgb + rbbg - brgb + brbg)\bar{b} + (2rrbg - 2rrgb \\
&+ rgrb - rgbr + grrb - grbr + rbgr - rbrg + brgr \\
&- brrg)\bar{r} + (2ggrb - 2ggbr - rggb + rgbg - grgb \\
&+ grbg + gbgr - gbrg + bggr - bgrg)\bar{g}\Big],
\end{aligned} \tag{4}$$

$$\begin{aligned}
\phi_2^P = \frac{1}{12}\Big[&(3bgbr - 3gbbr - 3brbg + 3rbbg - rbgb - 2rgbb \\
&+ 2grbb + brgb + gbrb - bgrb)\bar{b} + (3grrb - 3rgrb \\
&- 3brrg + 3rbrg - rbgr - 2gbrr + 2bgrr - grbr \\
&+ rgbr + brgr)\bar{r} + (3grgb - 3rggb + 3bggr - 3gbgr \\
&- grbg + rgbg + 2rbgg - 2brgg + gbrg - bgrg)\bar{g}\Big],
\end{aligned} \tag{5}$$

$$\phi_3^P = \frac{1}{3\sqrt{2}}\Big[(grbb - rgbb + rbgb - brgb + bgrb - gbrb)\bar{b} + (grbr - rgbr + rbgr - brgr + bgrr - gbrr)\bar{r} + (grbg - rgbg + rbgg - brgg + bgrg - gbrg)\bar{g}\Big]. \quad (6)$$

In the spin space, the direct product of five fermions represented in terms of Young tableau can be written as

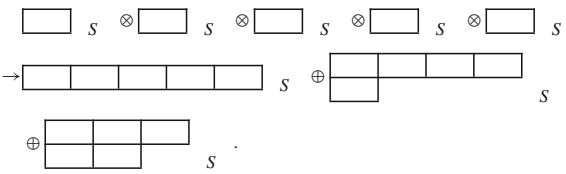

(7)

For the spin $J = 5/2, 3/2$ and $1/2$ of the pentaquarks, the configurations can be similarly represented in terms of Young tableau [5],[4,1], and [3,2] of one, four, and five dimensions. For the pentaquark with $J = 5/2$, we write the spin wavefunction as,

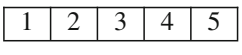

χ_1^P. (8)

In the case of the $J = 3/2$, the spin wavefunctions become

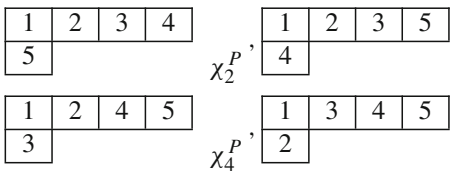

(9)

while for $J = 1/2$, they become,

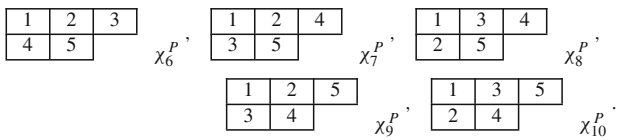

(10)

We see from the above analysis that to describe fully heavy pentaquarks $P_{Q_1Q_2Q_3Q_4\bar{Q}_5}$ with one antiquark $\bar{Q}_5$ having a given flavor and color, the antiquark can be temporarily omitted from the spin degrees of freedom. Thus, we shall identify the spin states shown in Eqs. (8) through (10) via the Young–Yamanouchi bases associated with the Young tableau [4], [3,1], and [2,2]. Given that the color and spin states represented in terms of the Young tableau respect certain symmetry, one can construct the combined color-spin state of a pentaquark which is fully antisymmetric under the exchange of any pair among the heavy quarks $1 = Q_1, 2 = Q_2, 3 = Q_3$, and $4 = Q_4$(for short).

We start from the color singlets in Eq. (3), and combine them with spin states by the outer product of the permutation group, S_4, resulting in the color $\otimes$ spin states for the quarks 1, 2, 3 and 4. After isolating spin of the antiquark, one can deduce the outer product between Young tableaux [2,1,1] of the color singlets and that of the spin states[4], [3,1], [2,2]. For the state expression in terms of the first four quarks (1234) mentioned above, one can obtain the Young tableau reps. of color $\otimes$ spin states and write them as that in Ref. [51] (see Eq. (17))

According to the method described in Ref. [52], all the possible Young–Yamanouchi bases (i.e. $\psi = \phi_2^P \chi_1^P$) for the pentaquarks we shall address in this work can be obtained from the couplings ($\otimes$) of the color and spin degrees of freedom. Collectively, we express these color-spin coupled bases, again, in terms of the Young tableau:

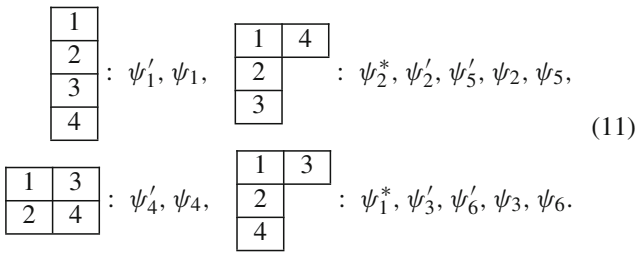

(11)

in which (for $J = 5/2$)

$$\psi_1^* = \phi_2^P \chi_1^P, \quad \psi_2^* = \phi_3^P \chi_1^P, \quad (12)$$

and (for $J = 3/2$)

$$\begin{aligned}
\psi_1' &= \frac{1}{\sqrt{3}}\phi_1^P \chi_5^P - \frac{1}{\sqrt{3}}\phi_2^P \chi_4^P + \frac{1}{\sqrt{3}}\phi_3^P \chi_3^P,\\
\psi_2' &= -\frac{1}{\sqrt{6}}\phi_1^P \chi_5^P + \frac{1}{\sqrt{6}}\phi_2^P \chi_4^P + \sqrt{\frac{2}{3}}\phi_3^P \chi_3^P,\\
\psi_3' &= \frac{1}{\sqrt{3}}\phi_1^P \chi_5^P - \frac{1}{\sqrt{6}}\phi_2^P \chi_3^P + \frac{1}{\sqrt{3}}\phi_2^P \chi_4^P + \frac{1}{\sqrt{6}}\phi_3^P \chi_4^P,\\
\psi_4' &= -\frac{1}{\sqrt{6}}\phi_1^P \chi_5^P - \frac{1}{\sqrt{3}}\phi_2^P \chi_3^P - \frac{1}{\sqrt{6}}\phi_2^P \chi_4^P + \frac{1}{\sqrt{3}}\phi_3^P \chi_4^P,\\
\psi_5' &= \phi_3^P \chi_2^P,\\
\psi_6' &= \phi_2^P \chi_2^P. \quad (13)
\end{aligned}$$

In the case of $J = 1/2$, the color $\otimes$ spin bases in Eq. (11) are explicitly,

$$\begin{aligned}
\psi_1 &= \frac{1}{\sqrt{3}}\phi_1^P \chi_8^P - \frac{1}{\sqrt{3}}\phi_2^P \chi_7^P + \frac{1}{\sqrt{3}}\phi_3^P \chi_6^P,\\
\psi_2 &= -\frac{1}{\sqrt{6}}\phi_1^P \chi_8^P + \frac{1}{\sqrt{6}}\phi_2^P \chi_7^P + \sqrt{\frac{2}{3}}\phi_3^P \chi_6^P,\\
\psi_3 &= \frac{1}{\sqrt{3}}\phi_1^P \chi_8^P - \frac{1}{\sqrt{6}}\phi_2^P \chi_6^P + \frac{1}{\sqrt{3}}\phi_2^P \chi_7^P + \frac{1}{\sqrt{6}}\phi_3^P \chi_7^P,\\
\psi_4 &= -\frac{1}{\sqrt{6}}\phi_1^P \chi_8^P - \frac{1}{\sqrt{3}}\phi_2^P \chi_6^P - \frac{1}{\sqrt{6}}\phi_2^P \chi_7^P + \frac{1}{\sqrt{3}}\phi_3^P \chi_7^P,\\
\psi_5 &= \frac{1}{\sqrt{2}}\phi_1^P \chi_{10}^P - \frac{1}{\sqrt{2}}\phi_2^P \chi_9^P,
\end{aligned}$$

Table 1 Color-spin bases of pentaquarks $q_1q_2q_3q_4\bar{q}_5$ with J^P quantum number

$q_1q_2q_3q_4$	J^P	Color-spin bases
$bbbb$, $cccc$	$3/2^-$	ψ_1'
	$1/2^-$	ψ_1
$bbbc$, $cccb$	$5/2^-$	ψ_2^*
	$3/2^-$	$\psi_1', \psi_2', \psi_5'$
	$1/2^-$	ψ_1, ψ_2, ψ_5
$ccbb$	$5/2^-$	$\sqrt{\frac{2}{3}}\psi_1^* - \sqrt{\frac{1}{3}}\psi_2^*$
	$3/2^-$	$\psi_1', \sqrt{\frac{2}{3}}\psi_3' - \sqrt{\frac{1}{3}}\psi_2', \psi_4', \sqrt{\frac{2}{3}}\psi_6' - \sqrt{\frac{1}{3}}\psi_5'$
	$1/2^-$	$\psi_1, \sqrt{\frac{2}{3}}\psi_3 - \sqrt{\frac{1}{3}}\psi_2, \psi_4, \sqrt{\frac{2}{3}}\psi_6 - \sqrt{\frac{1}{3}}\psi_5$

$$\psi_6 = \frac{1}{2}\phi_1^P \chi_{10}^P + \frac{1}{2}\phi_2^P \chi_9^P - \frac{1}{\sqrt{2}}\phi_3^P \chi_9^P . \tag{14}$$

Based on the Young tableau in Eq. (11) and Pauli principle for each pair of two fermions, we can construct all allowed color-spin wavefunctions and list them in Table 1 for pentaquarks consisting of four heavy quarks and a heavy antiquark. Based on similar principle, one can construct the states involved in chromomagnetic interactions (CMI) (18) with the help of color and spin factors (19,20) via the color bases (3) and spin bases (8–10), respectively. Following Ref. [53], we shall use the scaling ratios of color factors to evaluate the matrices of the binding energy, as discussed in Sect. 3.

3 MIT bag model and CMI

MIT bag model describes hadron as a sphere bag containing confined valence quarks. The model also includes perturbative inter-quark interactions via considering the lowest-order gluon exchange among quarks, which is referred as chromomagnetic interaction [54,55]. Mass of hadrons for a bag of radius R is [54,55],

$$M(R) = \sum_i \omega_i + \frac{4}{3}\pi R^3 B - \frac{Z_0}{R} + M_{BD} + M_{CMI}, \tag{15}$$

$$\omega_i = \left(m_i^2 + \frac{x_i^2}{R^2}\right)^{1/2}, \tag{16}$$

where the first term is total sum of the kinematic energy of relativistic quark i with mass m_i, the second is bag volume energy with B the bag constant, the third is zero point energy with coefficient Z_0, the forth is binding energy (M_{BD}) between heavy quarks or between heavy and strange quarks [56,57], and the fifth is chromomagnetic interaction. In Eq. (15), the bag radius R is bag radius to be determined variationally, and the quark momentum x_i in unit of R^{-1} satisfies a boundary condition on bag surface,

$$\tan x_i = \frac{x_i}{1 - m_i R - \left(m_i^2 R^2 + x_i^2\right)^{1/2}}, \tag{17}$$

which is to be solved iteratively in this work.

The interaction in this work enters among quarks via two parts, $\Delta M = M_{BD} + M_{CMI}$. The first part, the binding energy $M_{BD} = \sum_{M<N} B_{MN}$ ($M, N = s, c$ and b), proposed in Refs. [56,57], rises mainly from short-range chromoelectric interactions between heavy quarks or within heavy-strange pairs as they are (relatively) massive and move nonrelativistically. This part was supported by our previous work [53], which reconciles bag dynamics of the light and heavy hadrons. Five binding energies B_{cs}, B_{cc}, B_{bs}, B_{bc} and B_{bb} in the color $\bar{3}_c$ rep., extracted from the bag mass corrections to the baryons when heavy pairs (cs, cc, bs, bc and bb) involved, can be scaled to the binding energies B_{MN} in 6_c reps. via scaling factor ratios between two reps. [53,56]. As there are two reps. ($\bar{3}_c$ and 6_c) for color wavefunctions of quark pairs, as discussed in Sect. 2, the binding energies could be matrices in color-spin space given in Table 1, where spin bases are orthogonal.

The second part of interaction in Eq. (15) is chromomagnetic interaction M_{CMI}, which can be due to the short-range gluon exchange [58]. Similar to the interaction of magnetic moments of the quark spins, this part has the form of

$$M_{CMI} = -\sum_{i<j} \left(\lambda_i \cdot \lambda_j\right)\left(\sigma_i \cdot \sigma_j\right) C_{ij}, \tag{18}$$

where i and j denote the quark (anti-quark) indices, λ the Gell-Mann matrices, σ the Pauli matrices, and C_{ij} the coupling parameters of the CMI.

To compute the color and spin factor in Eq. (18), we employ the following formula of the matrix element:

$$\left\langle \lambda_i \cdot \lambda_j \right\rangle_{nm} = \sum_{\alpha=1}^{8} \mathrm{Tr}\left(c_{in}^\dagger \lambda^\alpha c_{im}\right) \mathrm{Tr}\left(c_{jn}^\dagger \lambda^\alpha c_{jm}\right), \tag{19}$$

$$\left\langle \sigma_i \cdot \sigma_j \right\rangle_{xy} = \sum_{\alpha=1}^{3} \mathrm{Tr}\left(\chi_{ix}^\dagger \sigma^\alpha \chi_{iy}\right) \mathrm{Tr}\left(\chi_{jx}^\dagger \sigma^\alpha \chi_{jy}\right), \tag{20}$$

where n, m and x, y indicate components of the basis vectors of color and spin wavefunctions of a hadron, respectively. The symbols c and χ denote bases of color and spin vectors associated with a quark, respectively. The matrices of two factors can be calculated with the help of Eqs. (19)–(20) once color-spin wavefunctions $\psi = \sum \phi^P \chi^P$ were determined.

In the MIT bag model, the CMI parameter C_{ij} is known analytically, given by [54]

$$C_{ij} = 3\frac{\alpha_s(R)}{R^3}\bar{\mu}_i\bar{\mu}_j I_{ij}, \tag{21}$$

where the reduced magnetic moment $\bar{\mu}_i$ and the (running) strong coupling α_s are given by

$$\bar{\mu}_i = \frac{R}{6}\frac{4\alpha_i + 2\lambda_i - 3}{2\alpha_i\,(\alpha_i - 1) + \lambda_i}, \tag{22}$$

$$\alpha_s(R) = \frac{0.296}{ln\left[1 + (0.281R)^{-1}\right]}, \tag{23}$$

and

$$I_{ij} = 1 + 2\int_0^R \frac{dr}{r^4}\bar{\mu}_i\bar{\mu}_j = 1 + F(x_i, x_j). \tag{24}$$

Here, $\alpha_i = \omega_i R$ and $\lambda_i = m_i R$ [54]. The function of $\alpha_s(R)$ in Eq. (23) is discussed in Ref. [53]. The function $F(x_i, x_j)$ in Eq. (24) is rational in terms of parameters x_i and x_j,

$$\begin{aligned} F(x_i, x_j) = &\left(x_i\sin^2 x_i - \frac{3}{2}y_i\right)^{-1}\left(x_j\sin^2 x_j - \frac{3}{2}y_j\right)^{-1} \\ &\times\left\{-\frac{3}{2}y_i y_j - 2x_i x_j\sin^2 x_i\sin^2 x_j\right. \\ &+\frac{1}{2}x_i x_j\left[2x_i\mathrm{Si}(2x_i) + 2x_j\mathrm{Si}(2x_j)\right. \\ &-(x_i + x_j)\mathrm{Si}(2(x_i + x_j)) \\ &\left.\left.-(x_i - x_j)\mathrm{Si}(2(x_i - x_j))\right]\right\}, \end{aligned} \tag{25}$$

where $y_i = x_i - \sin(x_i)\cos(x_i)$ and

$$\mathrm{Si}(x) = \int_0^x \frac{\sin(t)}{t}dt. \tag{26}$$

From Eq. (22), one can write the magnetic moment μ_i of the quark (anti-quark) i as, in bag model,

$$\mu_i = Q_i\bar{\mu}_i = Q_i\frac{R}{6}\frac{4\alpha_i + 2\lambda_i - 3}{2\alpha_i\,(\alpha_i - 1) + \lambda_i}, \tag{27}$$

with electric charge Q_i. As a result, the magnetic moment of a hadron with color-spin wavefunction ψ is,

$$\mu = \left\langle\psi\left|\sum\nolimits_i g_i\mu_i S_{iz}\right|\psi\right\rangle, \tag{28}$$

where $g_i = 2$, and S_{iz} is the third component of spin of the individual quark i [59].

We shall calculate the magnetic moments of the pentaquarks in unit of the magnetic moment of the proton μ_p and further transform the obtained results into that in unit of μ_N with the help of measured proton magnetic moment $\mu_p = 2.79285\mu_N$ [60,61]. Note that Eq. (28) also holds true in the case of chromomagnetic mixing, for which one can expand ψ in terms of the color-spin bases to find magnetic moment by Eq. (28). For the spin wavefunctions in Sect. 2, one can derive each diagonal element of magnetic moment. The results are listed in Table 2 in detail.

For the model parameters, we use the values in our previous work [53] which reconcile dynamics of the light and heavy hadrons. These values are Z_0, the constant B and masses of the quarks (the nonstrange quarks $n = u, d$, the strange quark s, the charm quark c and the bottom quark b) in this work,

$$\left\{\begin{array}{ll} Z_0 = 1.83, & B^{1/4} = 0.145\,\mathrm{GeV}, \\ m_n = 0\,\mathrm{GeV}, & m_s = 0.279\,\mathrm{GeV}, \\ m_c = 1.641\,\mathrm{GeV}, & m_b = 5.093\,\mathrm{GeV}. \end{array}\right\} \tag{29}$$

Meanwhile, using the binding energies $B_{QQ'}$ for the quark pair QQ' in color antitriplet rep. [53],

$$\bar{3}_c:\left\{\begin{array}{l} B_{cs} = -0.025\,\mathrm{GeV},\ B_{cc} = -0.077\,\mathrm{GeV}, \\ B_{bs} = -0.032\,\mathrm{GeV},\ B_{bb} = -0.128\,\mathrm{GeV}, \\ B_{bc} = -0.101\,\mathrm{GeV}, \end{array}\right\} \tag{30}$$

one can obtain the corresponding values of the binding energies for color-$\mathbf{6}_c$ rep., via multiplying the color-factor ratios (scaling factors). The results of the binding energies between quark pairs (denoted in subscripts) are:

$$6_c:\left\{\begin{array}{l} B_{cs} = 0.013\,\mathrm{GeV},\ B_{cc} = 0.039\,\mathrm{GeV}, \\ B_{bs} = 0.016\,\mathrm{GeV},\ B_{bb} = 0.064\,\mathrm{GeV}, \\ B_{bc} = 0.051\,\mathrm{GeV}. \end{array}\right\} \tag{31}$$

Given the parameter inputs in Eqs. (29), (30) and (31), one can apply variational method to Eq. (15) to determine the bag radius R and the respective momentum x_i via Eq. (17) for a given hadron with color-spin wavefunction ψ, given in Table 1. It is then straightforward to calculate masses and magnetic moments of fully heavy pentaquarks we address in this work, as detailed in Sect. 4.

Table 2 Sum rule of magnetic moments for pentaquarks $q_1q_2q_3q_4\bar{q}_5$

Spin basis	μ
χ_1^P	$\mu_1 + \mu_2 + \mu_3 + \mu_4 + \mu_5$
χ_2^P	$\frac{9}{10}(\mu_1 + \mu_2 + \mu_3 + \mu_4) - \frac{3}{5}\mu_5$
χ_3^P	$\frac{5}{6}(\mu_1 + \mu_2 + \mu_3) - \frac{1}{2}\mu_4 + \mu_5$
χ_4^P	$\frac{2}{3}(\mu_1 + \mu_2) - \frac{1}{3}\mu_3 + \frac{5}{6}(\mu_4 + \mu_5)$
χ_5^P	$\mu_3 + \mu_4 + \mu_5$
χ_6^P	$\frac{5}{9}(\mu_1 + \mu_2 + \mu_3) - \frac{1}{3}(\mu_4 + \mu_5)$
χ_7^P	$\frac{4}{9}(\mu_1 + \mu_2) - \frac{2}{9}\mu_3 + \frac{2}{3}\mu_4 - \frac{1}{3}\mu_5$
χ_8^P	$\frac{2}{3}(\mu_3 + \mu_4) - \frac{1}{3}\mu_5$
χ_9^P	μ_5
χ_{10}^P	μ_5

4 Masses and magnetic moments of fully heavy hadrons

Before discussing fully heavy pentaquarks, we first consider triply (fully) heavy baryons, the fully heavy binding systems of three quarks, which include the five baryons Ω_{ccc}, Ω_{ccb}, Ω^*_{ccb}, Ω_{cbb}, Ω^*_{cbb} and Ω_{bbb}, as listed in Table 3. For these baryons, we apply the same framework of MIT bag model (15) with the inputs in Eqs. (29), (30) and (31) to compute

Table 3 Computed masses (MeV) of triply heavy baryons, compared to other works cited. Bag radius R_0 is in GeV^{-1}

References	Ω_{ccc}	Ω_{ccb}	Ω^*_{ccb}	Ω_{cbb}	Ω^*_{cbb}	Ω_{bbb}
R_0	4.22	3.75	3.83	3.18	3.31	2.59
M	4841	8112	8133	11373	11402	14626
[62]	4670±150	7410±130	7450±160	10300± 100	10540±110	13280±100
[63]	4720±120	–	8070±100	–	11350±150	14300±200
[64]	4760	7867	7963	11077	11167	14370
[65]	4760±60	7980±70	7980±70	11190± 80	11190±80	14370±80
[66]	4777	7984	8005	11139	11163	14276
[67]	4796±8±18	8007±9±20	8037±9±20	11195±8±20	11229±8±20	14366±9±20
[68]	4798	8004	8023	11200	11221	14396
[69]	4799	8018	8046	11214	11245	14398
[70]	4803	8018	8025	11280	11287	14569
[71]	4810±100	8020±80	8030±80	11220±80	11230±80	14430±90
[72]	4834	–	–	–	–	–
[73]	–	–	–	–	–	14788
[74]	4897	8262	8273	11546	11589	14688
[75]	4900±250	8150±300	–	11400± 300	–	14700±300
[76]	4930	8010	8030	11090	11120	14230
[77]	4965	8245	8265	11535	11554	14834
[78]	4990±140	8230±130	8230±130	11500± 110	11490±110	14830±100
[79]	5000	8190	–	–	–	14570

the mass M and the bag radii R_0 of the fully heavy baryons, with other works cited for comparison.

Given the color-spin bases [53] (see Eq. (15)), defined as $\phi^B\chi_1^B$ and $\phi^B\chi_2^B$ for $J^P = 3/2^+$ and $1/2^+$, respectively, the CMI matrices and binding energies are well determined. When pentaquarks included, the computed results could help us further understand the general features of fully heavy systems, as we shall discuss in Sect. 5.

In Table 3, the second and third rows present bag radii R_0 and masses of triplet heavy baryons, and the data followed rows present the masses (in unit of MeV) cited from various works. One sees that the predicted masses of the Ω_{ccc}, for instance, ranges from 4520 MeV to 5130 MeV for which various methods including QCD sum rules [62,63,71,78] are employed. Up to 610 MeV, our prediction is close to the prediction 4810 ± 100 MeV in Ref. [71]. The lattice QCD was also applied to study the Ω_{ccc} in Ref. [67], with the prediction of $4796 \pm 8 \pm 18$ MeV. Comparing with the bag model computation of the doubly heavy baryons and tetraquarks [53] and the fully charm tetraquarks $cc\bar{c}\bar{c}$ in Ref. [80], our results for fully heavy baryons and pentaquarks are reasonable, considering that the inputs of the parameters are fitted only from light baryons and heavy mesons.

Using the method described in Sects. 2 and 3, one can construct a total mass formula (15) for the fully heavy hadrons containing the CMI and binding energies and calculate masses, magnetic moments and eigenvectors for all fully heavy systems containing the fully heavy mesons, baryons and pentaquarks, especially of the ten pentaquarks $P_{bbbbb\bar{b}}$, $P_{bbbbb\bar{c}}$, $P_{ccccb\bar{b}}$, $P_{ccccc\bar{c}}$, $P_{bbbcb\bar{b}}$, $P_{bbbcb\bar{c}}$, $P_{cccbb\bar{b}}$, $P_{cccbb\bar{c}}$, $P_{ccbbb\bar{b}}$ and $P_{ccbbb\bar{c}}$, whose color-spin bases have been listed in Table 1. Among these heavy hadrons, more attention is given to fully bottom and charm systems, which attracts extensive attention [81–86].

In Table 4, we present our computed results for the masses and magnetic moments of the fully bottom system $P_{bbbbb\bar{b}}$ and the fully charm system $P_{ccccc\bar{c}}$, compared to other works via the CMI model [81] and constituent quark model [82], which adopt the same color-spin wavefunctions, and via the lattice-QCD inspired model [83] and the chiral quark model [84]. The comparison is also given with the predictions via the QCD sum rules [85,86]. Agreement of our predictions with that by the constituent quark model [82] is achieved. Given the masses of triply heavy baryons computed in Table 3 and that of the measured heavy mesons [60], one finds that our predicted masses of fully heavy pentaquarks are all above the thresholds of the heavy baryons and mesons, as shown in Fig. 1.

Further more, we examine the respective mass splittings ΔM between spin multiplets due to the lowest two quantum numbers J for the fully heavy mesons, tetraquarks and pentaquarks and show them collectively in Table 5. Here, $J = \{0, 1\}$ or $J = \{1/2, 3/2\}$. For the fully heavy systems with identical quarks, it is found that ΔM are suppressed

Table 4 Predicted spectra of pentaquarks $P_{bbbb\bar{b}}$ and $P_{cccc\bar{c}}$ with comparisons from various works. Bag radius R_0 is in GeV^{-1}. Masses are in GeV. Magnetic moments μ are in unit of μ_N

State	J^P	R_0	M	M [81]	M [82]	M [83]	M [84]	M [85]	M [86]	μ
$P_{bbbb\bar{b}}$	$3/2^-$	3.48	24.761	23.775	24.211	24.035	23.748–23.752	–	$21.60^{+0.73}_{-0.22}$	− 0.08
	$1/2^-$	3.53	24.770	23.821	24.248	24.035	23.810–23.814	23.91±0.15	–	− 0.14
$P_{cccc\bar{c}}$	$3/2^-$	4.99	8.229	7.864	8.145	8.095	–	–	$7.41^{+0.27}_{-0.31}$	0.50
	$1/2^-$	5.08	8.262	7.949	8.193	8.045	7.892–7.893	7.93±0.15	–	0.83

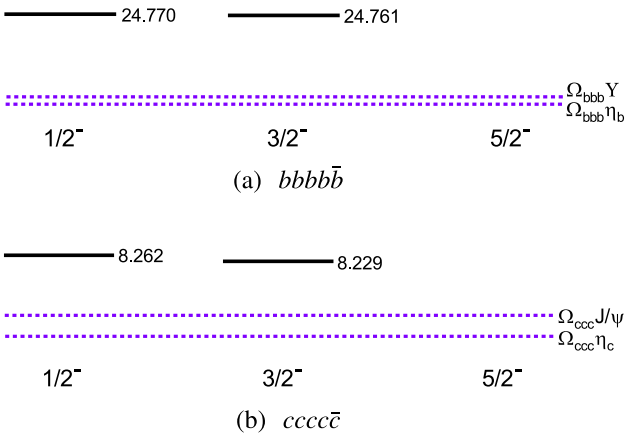

Fig. 1 Computed masses (in GeV, short solid lines) of pentaquarks $P_{bbbb\bar{b}}$ and $P_{cccc\bar{c}}$ for $J^P = 5/2^-, 3/2^-, 1/2^-$, compared to the respective thresholds plotted as long dotted lines

significantly with the heavy quark number N increasing and hadron becoming heavier. We see that the mass splittings are narrower for the bottom sector compared to the charm sector.

For the fully heavy pentaquarks with both bottom and charm flavors, we list the corresponding results computed via the MIT bag model in Tables 6, 7, 8, and 9, in comparison with other similar works cited [81,82]. The obtained masses are also compared to the respective thresholds and plotted in Fig. 2. All hadrons computed are above the thresholds associated with the baryons and mesons, meaning that these fully heavy pentaquarks are unstable against strong decays to two-hadron final states.

The instability of pentaquarks can be investigated by analyzing the eigenvectors obtained in this study. In order to examine the color-spin wavefunction ψ of pentaquark state, we utilize the corresponding eigenvectors and bases defined in Table 1, and express it in the form as shown below:

$$\psi = c_1\,(q_1q_2q_3)_{\mathbf{1}_c} \otimes (q_4\bar{q}_3)_{\mathbf{1}_c} + \ldots. \tag{32}$$

Here, c_1 represents the overlap between the wavefunctions of the pentaquark and the specific baryon ⊗ meson component, which corresponds to a scattering state. If the pentaquark state couples strongly to a scattering state, indicating that the probability $|c_1|^2$ of the collapse of ψ into a color-singlet (6) approaches 1, we can infer that it is unstable against strong decay with a very broad width.

For the pentaquark states presented in Tables 4 and 6, the values of $|c_1|^2$ are determined to be 1/3. Similarly, in Table 9, all the calculated values are approximately 1/3. Notably, the pentaquark states denoted by asterisks in Tables 7 and 8 have dominant components of scattering states with $|c_1|^2$ values greater than 0.83, while the remaining states range from 0.34 to 0.80. Based on the above discussions, we conclude that the pentaquark states $P_{bbbb\bar{Q}}$, $P_{cccc\bar{Q}}$, and $P_{ccbb\bar{Q}}$ ($Q = c, b$) are likely to possess a compact structure with relatively narrow widths. On the other hand, the bag radius R_0 ranging from $3.48\,\text{GeV}^{-1} = 0.7$ fm to $5.08\,\text{GeV}^{-1} = 1.0$ fm, which are in the order of the typical hadrons in size (about 1 fm), implies that these compact hadrons of pentaquarks may exist during hadronization in experiments of LHCb.

5 Mass pattern and linearity upon quark number

To explain the mass pattern obtained in this work, we consider question as to if the bag radius R leads to the larger volume energy $M_V = 4\pi R^3 B/3$ for the larger heavy quark number N, so that the hadron masses tend to be of suprathreshold. For this, we ignore the mass splittings due to the CMI and rewrite Eq. (15) in the form that hadrons consist of the identical flavor $Q(= c, b)$. The result is,

$$\bar{M}\,(R, N) = N\left(m_Q^2 + \frac{x_Q^2}{R^2}\right)^{1/2} + \frac{4}{3}\pi R^3 B - \frac{Z_0}{R} + N B_{QQ}, \tag{33}$$

where $\bar{M}$ stands for the spin-independent mass, N the total number of valence heavy quarks, and B_{QQ} the binding energy given in Eq. (30).

Owing to the scaling of the color factor, as mentioned in Sect. 3, the fully heavy hadrons with N identical quarks happen to have total binding energy of $N B_{QQ}$. Given Eq. (33), one can use it to examine each part of the energy for the fully heavy systems with identical quark number $N = 2 \sim 5$. The numerical results are listed in Table 10. One sees that the volume energy M_V grows quickly while the suppression of zero point energy $M_Z = -Z_0/R$ becomes weaker significantly

Table 5 Calculated masses M (in GeV) of fully heavy mesons [53], tetraquarks [80] and pentaquarks, with their mass splittings ΔM (in GeV) due to the lowest two J^P quantum numbers

$J^{P(C)}$	State	M	ΔM	State	M	ΔM
0^{-+}	η_c	3.002	0.095	η_b	9.396	0.064
1^{--}	J/ψ	3.097		Υ	9.460	
0^{++}	$cc\bar{c}\bar{c}$	6.469	0.050	$bb\bar{b}\bar{b}$	19.685	0.015
1^{+-}		6.519	0.053		19.700	0.017
0^{++}		6.572			19.717	
$1/2^-$	$ccc\bar{c}$	8.262	0.033	$bbb\bar{b}$	24.770	0.009
$3/2^-$		8.229			24.761	

Table 6 Predicted spectra of pentaquarks $P_{bbbb\bar{c}}$ and $P_{cccb\bar{c}}$ with comparisons from various works. Bag radius R_0 is in GeV^{-1}. Masses are in GeV. Magnetic moments μ are in unit of μ_N

State	J^P	R_0	M	M [81]	M [82]	μ
$P_{bbbb\bar{c}}$	$3/2^-$	3.89	21.472	20.652	20.975	− 0.65
	$1/2^-$	3.96	21.491	20.699	21.026	0.05
$P_{cccb\bar{c}}$	$3/2^-$	4.83	11.569	11.130	11.478	1.07
	$1/2^-$	4.86	11.582	11.177	11.502	0.63

Table 7 Predicted spectra of pentaquarks $P_{bbbc\bar{b}}$ and $P_{bbbc\bar{c}}$ with comparisons from various works. Bag radius R_0 is in GeV^{-1}. Masses are in GeV. Magnetic moments μ are in unit of μ_N. The states denoted by asterisks couple strongly to scattering states

J^P	$P_{bbbc\bar{b}}$						$P_{bbbc\bar{c}}$					
	R_0	Eigen vector	M	M [81]	M [82]	μ	R_0	Eigen vector	M	M [81]	M [82]	μ
$5/2^-$	3.92	1.00	21.480∗	20.648	–	0.31	4.28	1.00	18.183∗	17.407	–	− 0.26
$3/2^-$	3.93	(0.92, 0.21, 0.34)	21.484	20.654	21.092	0.13	4.26	(0.98, − 0.04, 0.17)	18.180	17.535	17.891	− 0.27
	3.90	(− 0.39, 0.70, 0.60)	21.475	20.644	–	0.35	4.23	(− 0.08, 0.75, 0.65)	18.171	17.406	–	0.05
	3.80	(− 0.11, − 0.68, 0.72)	21.451∗	20.578	–	− 0.21	4.16	(− 0.15, − 0.66, 0.74)	18.149∗	17.291	–	− 0.30
$1/2^-$	3.97	(− 0.99, − 0.10, 0.03)	21.493	20.691	21.079	− 0.03	4.32	(− 1.00, − 0.08, 0.07)	18.198	17.578	17.884	0.16
	3.89	(0.11, − 0.94, 0.31)	21.472	20.653	–	0.06	4.25	(0.10, − 0.88, 0.46)	18.177	17.523	–	0.16
	3.84	(0.00, 0.31, 0.95)	21.461	20.607	–	− 0.05	4.18	(0.02, 0.46, 0.89)	18.159	17.399	–	− 0.52

Table 8 Predicted spectra of pentaquarks $P_{cccb\bar{b}}$ and $P_{cccb\bar{c}}$ with comparisons from various works. Bag radius R_0 is in GeV^{-1}. Masses are in GeV. Magnetic moments μ are in unit of μ_N. The states denoted by asterisks couple strongly to scattering states

J^P	$P_{cccb\bar{b}}$						$P_{cccb\bar{c}}$					
	R_0	Eigen vector	M	M [81]	M [82]	μ	R_0	Eigen vector	M	M [81]	M [82]	μ
$5/2^-$	4.56	1.00	14.873∗	14.246	–	1.47	4.78	1.00	11.554∗	11.124	–	0.90
$3/2^-$	4.58	(− 0.89, 0.33, 0.32)	14.885	14.373	14.687	0.65	4.81	(− 0.42, 0.62, 0.67)	11.564	11.137	11.444	0.62
	4.56	(0.46, 0.65, 0.61)	14.873	14.246	–	1.08	4.77	(0.87, 0.49, 0.09)	11.549	11.101	–	0.59
	4.52	(0.01, − 0.69, 0.72)	14.862∗	14.182	–	1.31	4.70	(0.27, − 0.62, 0.74)	11.525∗	11.038	–	1.03
$1/2^-$	4.61	(0.97, − 0.22, 0.09)	14.895	14.411	14.676	0.27	4.86	(0.97, − 0.19, 0.14)	11.581	11.175	11.438	0.43
	4.56	(− 0.20, − 0.58, 0.79)	14.878	14.357	–	0.26	4.81	(− 0.23, − 0.68, 0.69)	11.564	11.137	–	0.17
	4.51	(0.11, 0.79, 0.61)	14.862	14.238	–	0.62	4.71	(0.04, 0.70, 0.71)	11.526	11.048	–	0.35

Table 9 Predicted spectra of pentaquarks $P_{ccbb\bar{b}}$ and $P_{ccbb\bar{c}}$ with comparisons from various works. Bag radius R_0 is in GeV^{-1}. Masses are in GeV. Magnetic moments μ are in unit of μ_N

J^P	$P_{ccbb\bar{b}}$						$P_{ccbb\bar{c}}$					
	R_0	Eigen vector	M	M [81]	M [82]	μ	R_0	Eigen vector	M	M [81]	M [82]	μ
$5/2^-$	4.27	1.00	18.182	17.477	–	0.88	4.55	1.00	14.872	14.295	–	0.32
$3/2^-$	4.29	(0.83, 0.36, − 0.13, 0.40)	18.191	17.554	17.785	0.28	4.57	(0.40, 0.63, − 0.26, 0.61)	14.880	14.375	14.579	− 0.01
	4.26	(− 0.54, 0.66, − 0.21, 0.47)	18.181	17.479	–	0.65	4.52	(− 0.86, 0.42, − 0.28, 0.01)	14.866	14.298	–	0.17
	4.22	(− 0.04, − 0.02, 0.92, 0.40)	18.170	17.457	–	0.65	4.51	(− 0.16, 0.28, 0.93, 0.20)	14.862	14.274	–	0.24
	4.20	(− 0.09, − 0.66, − 0.31, 0.68)	18.164	17.416	–	0.54	4.41	(− 0.26, − 0.59, − 0.04, 0.76)	14.828	14.197	–	0.36
$1/2^-$	4.32	(− 0.98, − 0.20, 0.03, 0.07)	18.200	17.576	17.785	0.08	4.61	(− 0.98, − 0.16, 0.01, 0.10)	14.893	14.406	14.566	0.26
	4.26	(0.20, − 0.85, 0.01, 0.49)	18.180	17.496	–	0.37	4.55	(0.19, − 0.81, − 0.06, 0.55)	14.875	14.318	–	0.31
	4.22	(− 0.03, 0.48, 0.30, 0.82)	18.168	17.437	–	0.41	4.48	(0.01, 0.48, 0.46, 0.75)	14.852	14.253	–	0.31
	4.16	(− 0.03, 0.14, − 0.95, 0.27)	18.154	17.405	–	− 0.06	4.39	(− 0.02, 0.30, − 0.89, 0.35)	14.821	14.185	–	− 0.07

with more valence quarks involved. This implies that fully heavy hadrons tend to be heavier when N becomes larger and they are all above thresholds of the decaying final states.

We further examine this mass pattern for fully heavy systems of the mesons, baryons, tetraquarks and pentaquarks within the same framework of MIT bag model. Beside the masses of baryons and pentaquarks which are computed via the MIT bag model, we cite the results for the mesons and tetraquarks in Refs. [53] and [80], respectively. The obtained results are plotted in Fig. 3. For the fully bottom and charm hadrons one sees that hadron masses rise almost linearly with N ranging from 2 to 5. It is notable that our mass predictions of the mesons and tetraquark $cc\bar{c}\bar{c}$ are in good agreements with experimental data, especially, the computed mass 6572 MeV of the fully charm tetraquark $cc\bar{c}\bar{c}$ agrees well with the measured mass $6552 \pm 10 \pm 12$ MeV of the newly-discovered resonance $X(6600)$ [8].

Inspired by Eq. (33) and the numerical results above, we promote the heavy quark number N to be as large as 20 mathematically, despite that a hadron with 20 valence quarks, if exist, may result in a very large and thereby unphysical bag radius R. We apply this procedure to $N = 2, 3, 4$ and 5 to test if the linear dependence of the hadron mass holds true as far as this work is involved. Similar to Fig. 3, we plot the numerical results in Fig. 4a for the spin-independent masses v.s. quark number N for fully bottom and charm systems respectively, with the data from $N = 2 \sim 20$. From these results, we find the following numerical fits for the fully bottom (denoted by subscript b) and charm (denoted by subscript c) systems (in GeV, $2 \leq N \leq 5$):

$$\begin{aligned} \bar{M}_b(N) &= 5.1004N - 0.7229, \\ \bar{M}_c(N) &= 1.7079N - 0.3241. \end{aligned} \tag{34}$$

In Fig. 4a, one observes the linear lines numerically, corresponding to Eq. (34), but the marching of it with the data of the spin-independent masses in Table 10 is approximated. To see this, we apply Eq. (33) to the fully light hadron systems with binding energy ignored, $B_{QQ} = 0$, and obtain the results plotted in Fig. 4b. The linear dependence breaks slightly when N is small, as it should be for the light hadrons. Notice that the (solid) line for the bottom sector is nearly linear in contrast with that for the charm sector, this implies that linearity of mass dependence holds true at heavy quark limit.

In the following, we show such a mass linearity upon N in heavy quark limit analytically. We expand the mass formula (33) in term of the inverse heavy-quark mass m_Q^{-1},

$$\begin{aligned} \bar{M}(R, N) \approx N m_Q \left(1 + \frac{x_Q^2}{2m_Q^2 R^2}\right) \\ + \frac{4}{3}\pi R^3 B - \frac{Z_0}{R} + N B_{QQ}, \end{aligned} \tag{35}$$

and minimize the mean mass Eq. (35) to find the bag radius,

$$\frac{\partial \bar{M}(R, N)}{\partial R} = 0 \Rightarrow R = R_0. \tag{36}$$

The solution of Eq. (36) in the large-N limit is $R_0 \sim N^{1/5}$. This gives rise to the following mass formula for fully heavy hadrons

$$\bar{M}(N) = N m_Q + \bar{\Lambda}_N + \frac{x_Q^2 N^{\frac{3}{5}}}{2m_Q}, \tag{37}$$

with $\bar{\Lambda}_N = N B_{QQ} + (4\pi B/3) N^{3/5} - Z_0 N^{-1/5}$, by analogy with the mass relation $m_{H_Q} = m_Q + \bar{\Lambda} + \frac{\Delta m^2}{2m_Q}$ in heavy quark effective theory (HQET). This explains the linear mass dependence of fully heavy hadrons with heavy quark flavor N, as demonstrated in Fig. 3.

6 Conclusions and remarks

In this work, we employ a unified framework of MIT bag model to perform a systematical study of all ground-state

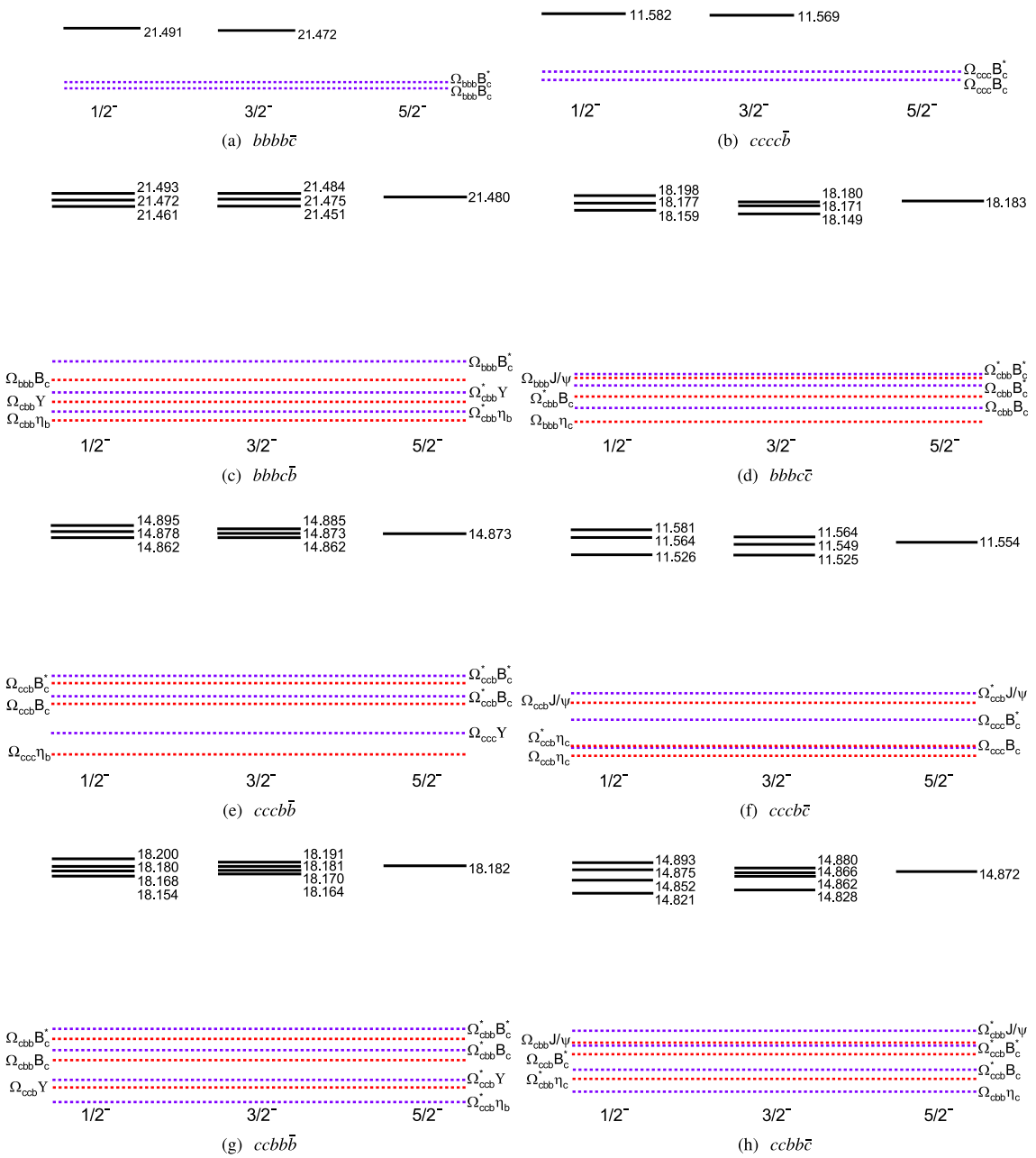

Fig. 2 Computed mass spectra (in GeV) of pentaquarks $P_{bbbb\bar{c}}$, $P_{cccc\bar{b}}$, $P_{bbbc\bar{b}}$, $P_{bbbc\bar{c}}$, $P_{cccb\bar{b}}$, $P_{cccb\bar{c}}$, $P_{ccbb\bar{b}}$, and $P_{ccbb\bar{c}}$ for $J^P = 5/2^-, 3/2^-, 1/2^-$, plotted by short solid lines, with respective threshold energy as blue (labeled right) and red (labeled left) dotted lines

configurations of fully heavy pentaquarks and other fully heavy hadrons. With the help of the color-spin wavefunctions of pentaquarks, which are classified via Young tableaux which respect symmetry of the $SU(2)_s \otimes SU(3)_c$ group and present in terms of the Young–Yamanouchi bases, we have computed the masses and magnetic moments of the fully charm, bottom and bottom-charm pentaquarks in ground states via numerical variational method that applies to the MIT bag model. Our computation predicts a set of masses of fully heavy pentaquarks, ranging from 8.229 GeV for the $P_{cccc\bar{c}}$ to 24.770 GeV for the $P_{bbbb\bar{b}}$. Combining with the similar bag-model computation of masses of fully heavy systems, we find that the masses of fully heavy hadrons (mesons, baryons, tetraquarks and pentaquarks) with identical flavors depend almost linearly upon the number N of the valence quarks in hadrons, and we demonstrate this linear behavior of the hadron masses using the MIT bag model, being consistent with the heavy quark symmetry at the heavy-quark limit. Our results also indicate that the heavier the fully heavy

Table 10 Numerical results for the mass components (all in GeV), the kinematic energy ω_Q (in GeV), the volume energy M_V, zero point energy M_Z and spin-independent mass $\bar{M}$ of fully heavy systems (mesons, baryons and pentaquarks) in detail. The parameters of the bag radius R_0 (GeV^{-1}) and x_Q are also shown for the heavy quark Q.

System	R_0	x_Q	ω_Q	M_V	M_Z	$\bar{M}$
$c\bar{c}$	3.45	2.886	1.842	0.076	−0.530	3.075
ccc	4.14	2.924	1.786	0.132	−0.442	4.818
$cc\bar{c}\bar{c}$	4.59	2.943	1.762	0.179	−0.399	6.520
$cccc\bar{c}$	4.92	2.955	1.748	0.220	−0.372	8.201
$b\bar{b}$	1.75	2.971	5.369	0.010	−1.047	9.445
bbb	2.54	3.022	5.230	0.030	−0.720	14.616
$bb\bar{b}\bar{b}$	3.07	3.042	5.188	0.054	−0.596	19.700
$bbbb\bar{b}$	3.45	3.053	5.169	0.076	−0.531	24.752

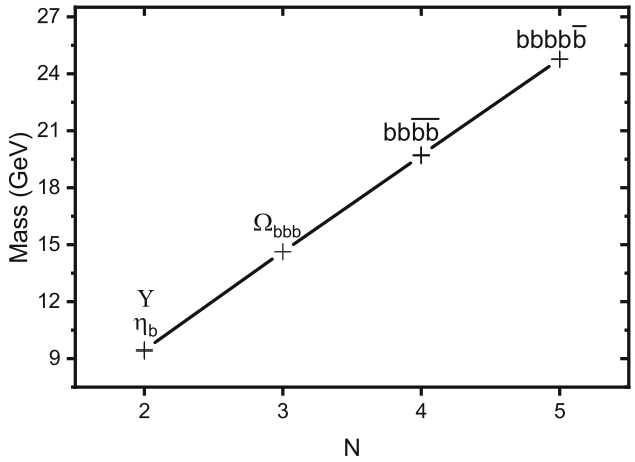

(a) fully bottom system

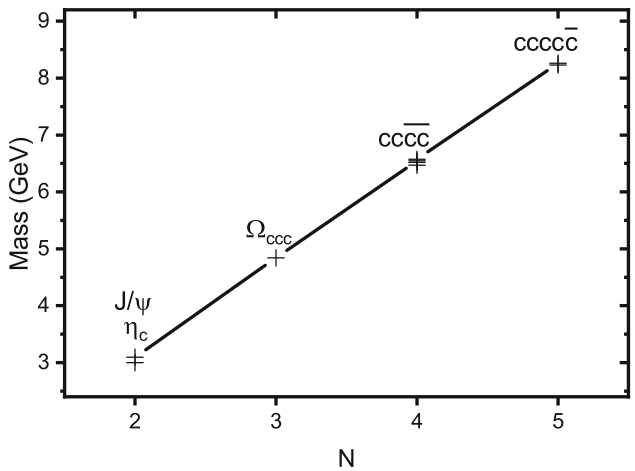

(b) fully charm system

Fig. 3 Masses of fully heavy systems ranging from mesons ($N = 2$) to pentaquarks ($N = 5$) with N the number of quarks and antiquarks, calculated in the unified framework of MIT bag model. The results of mesons are quoted from Ref. [53], and that of tetraquarks are from Ref. [80]

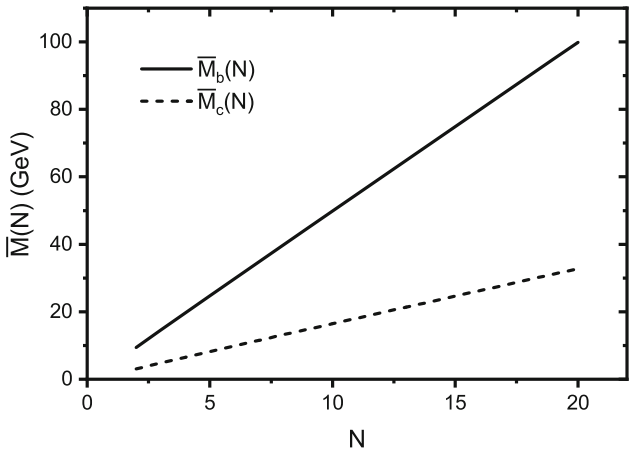

(a) fully heavy system

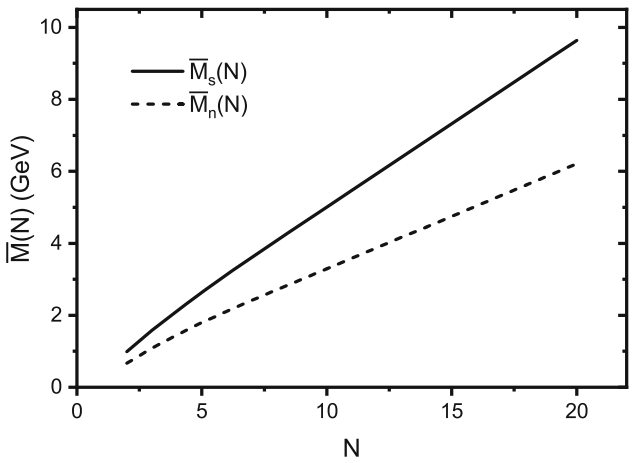

(b) fully light system

Fig. 4 The calculated spin-independent masses of fully heavy and light systems by Eq. (33). Quark number N is from 2 up to 20 for mathematical extrapolation

hadrons, the narrower the mass splittings of their lowest two multiplets (in J).

We remark that with the increase of the heavy quark number N, the bag radius R_0 of the fully heavy hadrons can rise up as high as 1 fm, and it results in the larger volume energy M_V and the less suppression of zero point energy M_Z, which makes them suprathreshold and unstable against strong decay. On the other hand, the shorter bag radius of the compact pentaquarks implies some larger possibilities for their formation via hadronization in experiments, compared to the formation of the hadrons containing light degrees of freedom. We hope that our predictions can help the future LHCb experiments to search the fully heavy pentaquarks or baryons addressed in this work.

Acknowledgements D. J. is supported by the National Natural Science Foundation of China under Grant No. 12165017.

Data Availability Statement This manuscript has associated data in a data repository. [Authors' comment: All data included in this manuscript are available up request by contacting the corresponding authors, group (e.g., PDG group) of collaboration or looking into the cited references.]

Funded by SCOAP[3]. SCOAP[3] supports the goals of the International Year of Basic Sciences for Sustainable Development.

References

1. M. Gell-Mann, Phys. Lett. **8**, 214 (1964). https://doi.org/10.1016/S0031-9163(64)92001-3
2. G. Zweig, CERN-TH-401 (1964)
3. R.L. Jaffe, Phys. Rev. D **15**, 267 (1977). https://doi.org/10.1103/PhysRevD.15.267
4. R.L. Jaffe, Phys. Rev. D **15**, 281 (1977). https://doi.org/10.1103/PhysRevD.15.281
5. S.K. Choi et al., Phys. Rev. Lett. **91**, 262001 (2003). https://doi.org/10.1103/PhysRevLett.91.262001
6. M. Ablikim et al., Phys. Rev. Lett. **110**, 252001 (2013). https://doi.org/10.1103/PhysRevLett.110.252001
7. E. Bouhova-Thacker, PoS **ICHEP2022**, 806 (2022). https://doi.org/10.22323/1.414.0806
8. J. Zhang, K. Yi, PoS **ICHEP2022**, 775 (2022). https://doi.org/10.22323/1.414.0775
9. R. Aaij et al., Sci. Bull. **65**(23), 1983 (2020). https://doi.org/10.1016/j.scib.2020.08.032
10. R. Aaij et al., Phys. Rev. Lett. **115**, 072001 (2015). https://doi.org/10.1103/PhysRevLett.115.072001
11. R. Aaij et al., Sci. Bull. **66**, 1278 (2021). https://doi.org/10.1016/j.scib.2021.02.030
12. [LHCb], CERN-EP-2022-198, LHCb-PAPER-2022-031 (2022)
13. L. Maiani, A.D. Polosa, V. Riquer, Phys. Lett. B **749**, 289 (2015). https://doi.org/10.1016/j.physletb.2015.08.008
14. R.F. Lebed, Phys. Lett. B **749**, 454 (2015). https://doi.org/10.1016/j.physletb.2015.08.032
15. V.V. Anisovich, M.A. Matveev, J. Nyiri, A.V. Sarantsev, A.N. Semenova (2015)
16. G.N. Li, X.G. He, M. He, JHEP **12**, 128 (2015). https://doi.org/10.1007/JHEP12(2015)128
17. R. Ghosh, A. Bhattacharya, B. Chakrabarti, Phys. Part. Nucl. Lett. **14**(4), 550 (2017). https://doi.org/10.1134/S1547477117040100
18. Z.G. Wang, Eur. Phys. J. C **76**(2), 70 (2016). https://doi.org/10.1140/epjc/s10052-016-3920-4
19. R. Zhu, C.F. Qiao, Phys. Lett. B **756**, 259 (2016). https://doi.org/10.1016/j.physletb.2016.03.022
20. J.M. Richard, A. Valcarce, J. Vijande, Phys. Lett. B **774**, 710 (2017). https://doi.org/10.1016/j.physletb.2017.10.036
21. Z.C. Yang, Z.F. Sun, J. He, X. Liu, S.L. Zhu, Chin. Phys. C **36**, 6 (2012). https://doi.org/10.1088/1674-1137/36/1/002
22. J.J. Wu, R. Molina, E. Oset, B.S. Zou, Phys. Rev. Lett. **105**, 232001 (2010). https://doi.org/10.1103/PhysRevLett.105.232001
23. J.J. Wu, T.S.H. Lee, B.S. Zou, Phys. Rev. C **85**, 044002 (2012). https://doi.org/10.1103/PhysRevC.85.044002
24. M. Karliner, J.L. Rosner, Phys. Rev. Lett. **115**(12), 122001 (2015). https://doi.org/10.1103/PhysRevLett.115.122001
25. I.W. Park, S. Cho, Y. Kim, S.H. Lee, Phys. Rev. D **105**(11), 114023 (2022). https://doi.org/10.1103/PhysRevD.105.114023
26. R. Chen, X. Liu, Phys. Rev. D **105**(1), 014029 (2022). https://doi.org/10.1103/PhysRevD.105.014029
27. T.J. Burns, E.S. Swanson, Eur. Phys. J. A **58**(4), 68 (2022). https://doi.org/10.1140/epja/s10050-022-00723-9
28. F. Yang, Y. Huang, H.Q. Zhu, Sci. China Phys. Mech. Astron. **64**(12), 121011 (2021). https://doi.org/10.1007/s11433-021-1796-0
29. P.P. Shi, F. Huang, W.L. Wang, Eur. Phys. J. A **57**(7), 237 (2021). https://doi.org/10.1140/epja/s10050-021-00542-4
30. M.W. Li, Z.W. Liu, Z.F. Sun, R. Chen, Phys. Rev. D **104**(5), 054016 (2021). https://doi.org/10.1103/PhysRevD.104.054016
31. X.Z. Ling, J.X. Lu, M.Z. Liu, L.S. Geng, Phys. Rev. D **104**(7), 074022 (2021). https://doi.org/10.1103/PhysRevD.104.074022
32. T.W. Wu, Y.W. Pan, M.Z. Liu, J.X. Lu, L.S. Geng, X.H. Liu, Phys. Rev. D **104**(9), 094032 (2021). https://doi.org/10.1103/PhysRevD.104.094032
33. W. Ruangyoo, K. Phumphan, C.C. Chen, A. Limphirat, Y. Yan, J. Phys. G **49**(7), 075001 (2022). https://doi.org/10.1088/1361-6471/ac58af
34. P. Ling, X.H. Dai, M.L. Du, Q. Wang, Eur. Phys. J. C **81**(9), 819 (2021). https://doi.org/10.1140/epjc/s10052-021-09613-8
35. J.X. Lu, M.Z. Liu, R.X. Shi, L.S. Geng, Phys. Rev. D **104**(3), 034022 (2021). https://doi.org/10.1103/PhysRevD.104.034022
36. Q. Wu, D.Y. Chen, R. Ji, Chin. Phys. Lett. **38**(7), 071301 (2021). https://doi.org/10.1088/0256-307X/38/7/071301
37. M.L. Du, V. Baru, F.K. Guo, C. Hanhart, U.G. Meißner, J.A. Oller, Q. Wang, JHEP **08**, 157 (2021). https://doi.org/10.1007/JHEP08(2021)157
38. C.W. Xiao, J.J. Wu, B.S. Zou, Phys. Rev. D **103**(5), 054016 (2021). https://doi.org/10.1103/PhysRevD.103.054016
39. J.T. Zhu, L.Q. Song, J. He, Phys. Rev. D **103**(7), 074007 (2021). https://doi.org/10.1103/PhysRevD.103.074007
40. R. Chen, Eur. Phys. J. C **81**(2), 122 (2021). https://doi.org/10.1140/epjc/s10052-021-08904-4
41. M.J. Yan, F.Z. Peng, M. Sánchez Sánchez, M. Pavon Valderrama, Eur. Phys. J. C **82**(6), 574 (2022). https://doi.org/10.1140/epjc/s10052-022-10522-7

42. G. Yang, J. Ping, Phys. Rev. D **95**(1), 014010 (2017). https://doi.org/10.1103/PhysRevD.95.014010
43. P. Yang, W. Chen, Chin. Phys. C **47**(1), 013105 (2023). https://doi.org/10.1088/1674-1137/ac9889
44. Y. Huang, H.Q. Zhu, Phys. Rev. D **104**(5), 056027 (2021). https://doi.org/10.1103/PhysRevD.104.056027
45. J.T. Zhu, S.Y. Kong, Y. Liu, J. He, Eur. Phys. J. C **80**(11), 1016 (2020). https://doi.org/10.1140/epjc/s10052-020-8410-z
46. G. Yang, J. Ping, J. Segovia, Phys. Rev. D **99**(1), 014035 (2019). https://doi.org/10.1103/PhysRevD.99.014035
47. T.J. Burns, Eur. Phys. J. A **51**(11), 152 (2015). https://doi.org/10.1140/epja/i2015-15152-6
48. H.X. Chen, W. Chen, X. Liu, S.L. Zhu, Phys. Rep. **639**, 1 (2016). https://doi.org/10.1016/j.physrep.2016.05.004
49. Y.R. Liu, H.X. Chen, W. Chen, X. Liu, S.L. Zhu, Prog. Part. Nucl. Phys. **107**, 237 (2019). https://doi.org/10.1016/j.ppnp.2019.04.003
50. N. Brambilla, S. Eidelman, C. Hanhart, A. Nefediev, C.P. Shen, C.E. Thomas, A. Vairo, C.Z. Yuan, Phys. Rep. **873**, 1 (2020). https://doi.org/10.1016/j.physrep.2020.05.001
51. H.T. An, K. Chen, Z.W. Liu, X. Liu, Phys. Rev. D **103**(11), 114027 (2021). https://doi.org/10.1103/PhysRevD.103.114027
52. F. Stancu, S. Pepin, Few Body Syst. **26**, 113 (1999). https://doi.org/10.1007/s006010050109
53. W.X. Zhang, H. Xu, D. Jia, Phys. Rev. D **104**(11), 114011 (2021). https://doi.org/10.1103/PhysRevD.104.114011
54. T.A. DeGrand, R.L. Jaffe, K. Johnson, J.E. Kiskis, Phys. Rev. D **12**, 2060 (1975). https://doi.org/10.1103/PhysRevD.12.2060
55. K. Johnson, Acta Phys. Polon. B **6**, 865 (1975)
56. M. Karliner, J.L. Rosner, Phys. Rev. D **90**(9), 094007 (2014). https://doi.org/10.1103/PhysRevD.90.094007
57. M. Karliner, J.L. Rosner, Nature **551**, 89 (2017). https://doi.org/10.1038/nature24289
58. A. De Rujula, H. Georgi, S.L. Glashow, Phys. Rev. D **12**, 147 (1975). https://doi.org/10.1103/PhysRevD.12.147
59. G.J. Wang, R. Chen, L. Ma, X. Liu, S.L. Zhu, Phys. Rev. D **94**(9), 094018 (2016). https://doi.org/10.1103/PhysRevD.94.094018
60. R.L. Workman et al., PTEP **2022**, 083C01 (2022). https://doi.org/10.1093/ptep/ptac097
61. E. Tiesinga, P.J. Mohr, D.B. Newell, B.N. Taylor, Rev. Mod. Phys. **93**(2), 025010 (2021). https://doi.org/10.1103/RevModPhys.93.025010
62. J.R. Zhang, M.Q. Huang, Phys. Lett. B **674**, 28 (2009). https://doi.org/10.1016/j.physletb.2009.02.056
63. T.M. Aliev, K. Azizi, M. Savcı, J. Phys. G **41**, 065003 (2014). https://doi.org/10.1088/0954-3899/41/6/065003
64. S.X. Qin, C.D. Roberts, S.M. Schmidt, Few Body Syst. **60**(2), 26 (2019). https://doi.org/10.1007/s00601-019-1488-x
65. A. Faessler, T. Gutsche, M.A. Ivanov, J.G. Korner, V.E. Lyubovitskij, D. Nicmorus, K. Pumsa-ard, Phys. Rev. D **73**, 094013 (2006). https://doi.org/10.1103/PhysRevD.73.094013
66. A. Bernotas, V. Simonis, Lith. J. Phys. **49**, 19 (2009). https://doi.org/10.3952/lithjphys.49110
67. Z.S. Brown, W. Detmold, S. Meinel, K. Orginos, Phys. Rev. D **90**(9), 094507 (2014). https://doi.org/10.1103/PhysRevD.90.094507
68. G. Yang, J. Ping, P.G. Ortega, J. Segovia, Chin. Phys. C **44**(2), 023102 (2020). https://doi.org/10.1088/1674-1137/44/2/023102
69. J.M. Flynn, E. Hernandez, J. Nieves, Phys. Rev. D **85**, 014012 (2012). https://doi.org/10.1103/PhysRevD.85.014012
70. A.P. Martynenko, Phys. Lett. B **663**, 317 (2008). https://doi.org/10.1016/j.physletb.2008.04.030
71. Z.G. Wang, AAPPS Bull. **31**, 5 (2021). https://doi.org/10.1007/s43673-021-00006-3
72. K.W. Wei, B. Chen, X.H. Guo, Phys. Rev. D **92**(7), 076008 (2015). https://doi.org/10.1103/PhysRevD.92.076008
73. K.W. Wei, B. Chen, N. Liu, Q.Q. Wang, X.H. Guo, Phys. Rev. D **95**(11), 116005 (2017). https://doi.org/10.1103/PhysRevD.95.116005
74. B. Patel, A. Majethiya, P.C. Vinodkumar, Pramana **72**, 679 (2009). https://doi.org/10.1007/s12043-009-0061-4
75. F.J. Llanes-Estrada, O.I. Pavlova, R. Williams, Acta Phys. Polon. Suppl. **6**(3), 821 (2013). https://doi.org/10.5506/APhysPolBSupp.6.821
76. L.X. Gutiérrez-Guerrero, A. Bashir, M.A. Bedolla, E. Santopinto, Phys. Rev. D **100**(11), 114032 (2019). https://doi.org/10.1103/PhysRevD.100.114032
77. W. Roberts, M. Pervin, Int. J. Mod. Phys. A **23**, 2817 (2008). https://doi.org/10.1142/S0217751X08041219
78. Z.G. Wang, Commun. Theor. Phys. **58**, 723 (2012). https://doi.org/10.1088/0253-6102/58/5/17
79. P.L. Yin, C. Chen, G.a. Krein, C.D. Roberts, J. Segovia, S.S. Xu, Phys. Rev. D **100**(3), 034008 (2019). https://doi.org/10.1103/PhysRevD.100.034008
80. T.Q. Yan, W.X. Zhang, D. Jia (2023)
81. H.T. An, K. Chen, Z.W. Liu, X. Liu, Phys. Rev. D **103**(7), 074006 (2021). https://doi.org/10.1103/PhysRevD.103.074006
82. H.T. An, S.Q. Luo, Z.W. Liu, X. Liu, Phys. Rev. D **105**(7), 074032 (2022). https://doi.org/10.1103/PhysRevD.105.074032
83. G. Yang, J. Ping, J. Segovia, Phys. Rev. D **106**(1), 014005 (2022). https://doi.org/10.1103/PhysRevD.106.014005
84. Y. Yan, Y. Wu, X. Hu, H. Huang, J. Ping, Phys. Rev. D **105**(1), 014027 (2022). https://doi.org/10.1103/PhysRevD.105.014027
85. Z.G. Wang, Nucl. Phys. B **973**, 115579 (2021). https://doi.org/10.1016/j.nuclphysb.2021.115579
86. J.R. Zhang, Phys. Rev. D **103**(7), 074016 (2021). https://doi.org/10.1103/PhysRevD.103.074016